Insight into the key aspects of the regeneration process in the NO_x storage reduction (NSR) reaction probed using fast transient kinetics coupled with isotopically labelled ^{15}NO over Pt and Rh-containing Ba/Al_2O_3 catalysts

J.P. Breen [*], R. Burch, C. Fontaine-Gautrelet, C. Hardacre, C. Rioche

CenTACat, School of Chemistry and Chemical Engineering, Queen's University Belfast, Belfast BT9 5AG, United Kingdom

Abstract

For the first time, the coupling of fast transient kinetic switching and the use of an isotopically labelled reactant (^{15}NO) has allowed detailed analysis of the evolution of all the products and reactants involved in the regeneration of a NO_x storage reduction (NSR) material. Using realistic regeneration times (ca. 1 s) for Pt, Rh and Pt/Rh-containing Ba/Al_2O_3 catalysts we have revealed an unexpected double peak in the evolution of nitrogen. The first peak occurred immediately on switching from lean to rich conditions, while the second peak started at the point at which the gases switched from rich to lean. The first evolution of nitrogen occurs as a result of the fast reaction between H_2 and/or CO and NO on reduced Rh and/or Pt sites. The second N_2 peak which occurs upon removal of the rich phase can be explained by reaction of stored ammonia with stored NO_x, gas phase NO_x or O_2. The ammonia can be formed either by hydrolysis of isocyanates or by direct reaction of NO and H_2.

The study highlights the importance of the relative rates of regeneration and storage in determining the overall performance of the catalysts. The performance of the monometallic 1.1%$Rh/Ba/Al_2O_3$ catalyst at 250 and 350 °C was found to be dependent on the rate of NO_x storage, since the rate of regeneration was sufficient to remove the NO_x stored in the lean phase. In contrast, for the monometallic 1.6%$Pt/Ba/Al_2O_3$ catalyst at 250 °C, the rate of regeneration was the determining factor with the result that the amount of NO_x stored on the catalyst deteriorated from cycle to cycle until the amount of NO_x stored in the lean phase matched the NO_x reduced in the rich phase. On the basis of the ratio of exposed metal surface atoms to total Ba content, the monometallic 1.6%$Pt/Ba/Al_2O_3$ catalyst outperformed the Rh-containing catalysts at 250 and 350 °C even when CO was used as a reductant.

© 2007 Elsevier B.V. All rights reserved.

Keywords: NO_x storage reduction; NSR; Barium; Platinum; Rhodium; Regeneration; Isotopically labelled ^{15}NO; Fast transient kinetics; CO; H_2

1. Introduction

NO_x storage and reduction (NSR) catalysts are considered to be one of the most promising solutions to the problem of NO_x removal from lean burn engine exhausts. The NSR concept was introduced by Toyota in the mid 90s for automotive emission control [1]. It is a simple concept in which NO_x is trapped under lean conditions (for 60–120 s) and then reduced to N_2 during a short rich period (of ca. 1 s). A typical catalyst consists of a support material (often alumina), precious metals (usually a combination of Pt and Rh) and an alkali or alkaline-earth metal oxide or carbonate (typically barium oxide and/or carbonate)

which acts as the NO_x storage material. Although the concept is simple, the understanding of the mechanisms and processes underlying the basic process has been difficult to disentangle. Burch [2] has commented on the apparently contradictory results that have been obtained in the literature, and this has been reinforced in a more recent study by Lesage et al. [3]. These authors illustrate the divergent views on the mechanism of NO_x storage and reduction and Burch makes the point that the various conclusions are most probably correct but that the variety of conditions and materials used makes it difficult to obtain any clear understanding of the processes and mechanisms involved in a realistic NSR environment.

In order to avoid these problems, several groups have undertaken the study of the NSR reaction using materials and conditions more closely approximating those encountered in a real lean burn exhaust system. For example, several researchers

---

* Corresponding author.
  E-mail address: j.breen@qub.ac.uk (J.P. Breen).

have emphasised the need to have both water and CO_2 present [4–6], and Takahashi et al. [7] have pointed out the importance of using realistic rich regeneration times. Thus, while a number of studies have used realistic storage periods of 1–2 min, the majority of regeneration studies have used very long times compared to the ca. 1 s typically used in real systems. A number of researchers have managed to approach realistic regeneration times by using periods ranging from 1.5 to 5 s [7–11,14]. More recently, temporal analysis of products (TAP) techniques have been employed to study the regeneration and storage under fast transient conditions but with the disadvantage that the catalyst is exposed to the reaction mix under vacuum conditions [12,13]. James et al. [14] have probed the storage/regeneration reaction using a pulsed flow reactor in which pulses of NO were alternated with pulses of reductant.

In a recent study [15], we have reported the development of a fast switching and analysis apparatus capable of allowing regeneration periods of ca. 1 s to be achieved. To exemplify the value of this system the performance of a 1%Pt/17.5%Ba/γ-Al_2O_3 NSR catalyst was studied as a function of the temperature, rich phase duration, reductant concentration, the type of reductant and the effect of an inert gas purge. It was found that short regeneration times, low concentrations of reductant and low temperatures resulted in a decrease in NSR catalyst performance over the course of several cycles. This was attributed to incomplete regeneration of the catalyst, and it was found that readsorption of NO_x released during the rich phase but not reduced quickly enough can be a significant cause of loss of catalyst performance. The study underlined the importance of the regeneration step in the NSR process. The results of this earlier study [15] led us to investigate the regeneration process in more detail.

For the regeneration step, different parameters such as the gas composition, the type of noble metal and the temperature have been investigated. Many authors have noted that, for Pt based NSR catalysts, H_2 is a more effective reductant than CO [7,14–21]. This is especially apparent at low temperatures. On the other hand, Cant and Patterson [22] noted that CO was a more effective reductant than H_2. However, their experiments were carried out under dry conditions over a BaO/Al_2O_3 catalyst.

The mechanism of the reduction process has been investigated by a number of authors. Lesage et al. [23] used FTIR analysis to study the regeneration reaction with H_2 and CO. They found that during reduction with CO isocyanates form on the oxide components of the catalyst, and these then readily react with water to form CO_2 and NH_3. In addition to hydrolysis, the isocyanates could be selectively oxidised by oxygen to nitrogen and carbon dioxide. Szailer et al. [24] also used FTIR analysis to study the regeneration and reported findings similar to Lesage et al. They invoked a complex reaction mechanism whereby surface oxygen atoms are removed by either H_2 or CO, allowing direct reduction of stored NO_x with H_2 and the reaction between CO and surface N atoms to form NCO which is subsequently hydrolysed. The direct reaction of NCO with decomposing NO_x to form N_2 was also invoked as a possibility at high temperatures.

In addition to platinum, it is suggested that the addition of rhodium to the NSR catalyst formulation improves the regeneration and the overall catalyst efficiency [25]. Despite the fact that Rh is an important component of commercial NSR catalysts, there have been few studies on the role of Rh in the trapping/regeneration process. Skoglundh and co-workers [17,26,27] have carried out a comparative study of the regeneration of PM/BaO/Al_2O_3 catalysts (PM = Pt, Pd or Rh). They found that the type of precious metal affects the NO_x storage properties; in particular they found that Rh/BaO/Al_2O_3 shows good reduction ability but relatively low NO_x storage capacity. They also found that the use of CO as a reducing agent instead of H_2 resulted in a lower NO_x reduction capacity for the Pt/$BaCO_3$/Al_2O_3 catalyst in comparison to the corresponding Rh based sample. In these studies, the regeneration time was of the order of 5 min and trapping time up to 40 min so, as we found earlier [15] some of the subtleties of the regeneration may be lost.

The present study aims to investigate the role of Pt and Rh in the regeneration process under realistic NSR conditions. The combination of the fast transient kinetic switching, apparatus and the use of isotopically labelled ^{15}NO has for the first time allowed the monitoring of all reactants and products in a full gas mix with good temporal resolution. In particular, it allows for the nitrogen to be traced as it is formed; this is typically not possible due to IR invisibility or overlap with fragments of CO and CO_2 when using mass spectroscopy and ^{14}NO as the feed.

2. Experimental

2.1. Catalyst preparation

The nominal 0.5 wt%Pt/17.5 wt%Ba/γ-Al_2O_3 catalyst (0.5Pt) was prepared by wet impregnation of a commercial γ-Al_2O_3 (BET surface area: 238 m^2 g^{-1}) using appropriate concentrations of solutions of dinitrodiamino Pt (Pt/DNDA) and Ba$(NO_3)_2$. The γ-Al_2O_3 support was calcined at 500 °C for 2 h prior to impregnation. This base catalyst was then used to make further Pt and Rh catalysts by impregnation using the appropriate concentration of solutions of dinitrodiamino Pt (Pt/DNDA) or Rh$(NO_3)_3$ to give a monometallic higher loading Pt/Ba/γ-Al_2O_3 catalyst and a bimetallic Pt/Rh/Ba/γ-Al_2O_3 catalyst. The nominal 1.1 wt%Rh/17.5 wt%Ba/γ-Al_2O_3 catalyst (1.1Rh) was prepared by impregnation as above. After each impregnation, the catalyst was reduced at 500 °C for 2 h under 4% H_2 in helium and calcined at 500 °C for 2 h. The metal loadings were selected in order to have monometallic Pt and Rh catalysts and a bimetallic Pt/Rh catalyst with similar molar concentrations of metal in each case. The metal loading of each sample was determined by ICP analysis.

2.2. Experimental method

The catalysts were evaluated using a fast transient kinetic apparatus described in more detail elsewhere [15]. The apparatus allows a rich period as short as 1.2 s to be utilised. The valve switching and flow controller settings were computer

controlled using a LabVIEW program developed in-house. The overall time resolution for data acquisition is better than 150 ms. The time taken to switch 90% of one feed to the other is of the order of ~200 ms. The bench flow reactor consisted of a quartz tube enclosed in an electric furnace. The gas mixtures used to simulate the exhaust were introduced using Aera mass flow controllers with the exception of the steam which was supplied using a Bronkhorst controlled evaporator mixer. Gas analysis was performed using a Hiden HPR 20 quadrupole mass spectrometer. The MS capillary inlet and a type K thermocouple were located at the outlet of the catalyst bed.

For the gas feed, [14]NO or [15]NO were used; in some instances the initial cycles were carried out using [14]NO and the latter ones with [15]NO. This was done to avoid wasting [15]NO during periods in which the catalyst was coming to steady state. The use of both [15]NO and [14]NO allowed analysis of all the products of reaction in a full gas mix. Using [14]NO it was possible to monitor the evolution of [14]NO (m/e = 30) and [14]NH containing species (m/e = 15). The signal at m/e = 15 can be attributed to the [14]NH fragment of [14]NH$_3$. Overlap with fragments due to H_2O at m/e = 17 and O_2 (and H_2O) at m/e = 16 prevented the use of either of these mass to charge ratios for tracking NH$_3$. [15]NO allowed the evolution of [15]NO (m/e = 31), [15]N$_2$ (m/e = 30), [15]N$_2$O (m/e = 46) and [15]NO$_2$ (m/e = 47) to be tracked without interference from fragments associated with CO (m/e = 28) and CO_2 (m/e = 44). Kr (m/e = 84) was also monitored. Krypton was used as an internal standard as well as an internal marker to differentiate between the gas mixtures.

The amount of NO was quantified using the ratio (m/e 30)/(m/e 84) for [14]NO to Kr or the ratio (m/e 31)/(m/e 84) for [15]NO to Kr and by measuring a known level of NO in the feed (through a bypass) for each experiment. The baseline was measured for each gas before each experiment. The percentage of NO$_x$ stored during the lean phase was calculated using the following expression:

$$NO_{x\,stored}\,(\%) = \left(\frac{[NO_x]_{stored}}{[NO_x]_{in}} \right) \times 100$$
$$= \left(\frac{[NO_x]_{in} - [NO_x]_{out}}{[NO_x]_{in}} \right) \times 100$$

where: $[NO_x]$ = number of moles of NO$_x$

The mass spectrometer was calibrated for nitrogen, nitrous oxide and ammonia using various dilutions of 1% N_2/Ar, 1% NH$_3$/Ar and 0.4% N_2O/Ar, respectively. It was found that the relative ratios of the fragments of nitrogen, nitrous oxide and ammonia at m/e = 28, 44 and 15 for a given concentration was 10.1:4.3:1, respectively. For quantification of products during regeneration it is assumed that during the section of cycles during which NO$_x$ stored does not vary from cycle to cycle (typically after approximately 18 cycles) all the NO$_x$ stored in the preceding cycle is released as nitrogen, ammonia and nitrous oxide during regeneration. The response factors of the fragments for ammonia, nitrogen and nitrous oxide are used to determine the relative quantities of products produced during the regeneration.

Table 1
Composition of the different gas mixtures

	Lean	Rich
H_2O	10%	10%
CO_2	10%	10%
O_2	5%	–
NO	300 ppm	–
H_2	–	1.5 or 6.0%
CO	–	0 or 4.5%
Kr	2%	–
Ar	Balance	Balance

2.3. Typical experiments

In each experiment, two reaction mixtures were alternated in a predefined sequence. The different mixtures are summarized in Table 1.

Water and CO_2 were always included in the feed as these compounds are always present in exhaust gases. The experiments were all carried out with a total flow rate of 200 cm^3 min^{-1} and a catalyst mass of 50 mg; giving a space velocity of 240,000 cm^3 g^{-1} h^{-1} and an average contact time of ~0.012 s. The temperature was maintained at 250 or 350 °C. Before each experiment the catalyst was pretreated for 5 min in the rich mixture, followed by a 1 min purge, 10 min in the lean mixture without NO$_x$ and finally a 1 min purge. This sequence normalised the state of the catalyst for each experiment and allowed the baseline to be measured with each gas mixture.

Theoretically, the amount of reductant introduced in 1.2 s was just sufficient to reduce all the NO$_x$ stored in 60 s as nitrates if this was fully converted to ammonia. However, this is very clearly an unrealistic worst case scenario, where all the NO$_x$ is stored and all of it is converted to ammonia. In practice it was found that 100% NO$_x$ was never stored (in the first or subsequent cycles) and that in all cases the selectivity to ammonia was a lot less than 100% (so that much less reductant would be required for reduction). Potential loses of reductant are combustion at the lean/rich interface and surface reduction of the PGM oxides to the corresponding metal. However, the data in Fig. 1 showing about 95% storage of NO$_x$ over more than 40 cycles for the 1.6Pt catalyst suggest that the amount of reductant is not a limiting factor during regeneration.

3. Results

3.1. Catalyst characterisation

Table 2 shows that the 0.5Pt0.8Rh and 1.1Rh catalysts have almost identical molar concentrations of metal (103 ± 1 μmol/g$_{cat}$). The 1.6Pt catalyst has a lower molar loading of precious metal of 81 μmol/g$_{cat}$. The ratio of adsorbed CO to Pt and/or Rh is also given in Table 2. CO chemisorptions are often used to calculate metallic dispersions; however, due to the fact that one of the catalysts is bimetallic and that the adsorption stoichiometry for Rh in particular can vary between 1 and 2 depending on particle size [28], no attempt is made here to derive metallic surface areas. However, it is evident (from the
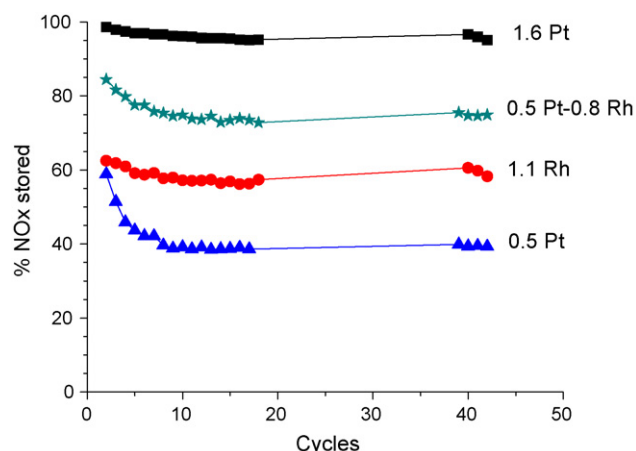
Fig. 1. %NO_x stored as a function of the number of 60 s lean/1.2 s rich cycles with 1.5% H_2 + 4.5% CO reductant mix.

Fig. 2. NO_x evolution as a function of time during a 60 s lean/1.2 s rich cycle, cycle number 40.

ratio M*/CO) that the Rh-containing catalysts can store significantly greater quantities of CO than the monometallic Pt catalysts.

3.2. Catalytic results at 350 °C

The NO_x storage performance of the Pt and/or Rh containing NSR catalysts were tested at 350 °C over the course of more than 40 lean/rich cycles. Fig. 1 shows the percentage NO_x stored during these cycles. For the initial 18 cycles, during which time the catalysts tended to show decreasing NO_x storage performance, [14]NO was used as a feed gas. In order to observe the evolution of gas phase products, in particular N_2, the feed gas was then switched to [15]NO. The time taken to completely purge [14]NO from the catalyst was ∼20 cycles. The data points obtained after ∼38 cycles were calculated solely on the basis of [15]NO storage and show very similar values to those obtained using [14]NO after 18 cycles, indicating that there is no change in performance over the course of these latter cycles.

The 1.1Rh and 0.5Pt catalysts show similar initial NO_x storage of ∼60%. However, the performance of the 0.5Pt catalyst decreased significantly over time giving a final NO_x storage of 40%. The performance of 1.1Rh remained relatively constant. The addition of 0.8Rh to the 0.5Pt results in a catalyst (0.5Pt0.8Rh, containing 102 µmol/g$_{cat}$ of metal) with a higher activity than 1.1Rh, although deactivation is evident as the amount of NO_x stored decreases from 85 to 75% over the course of 10 cycles, remaining constant thereafter. The
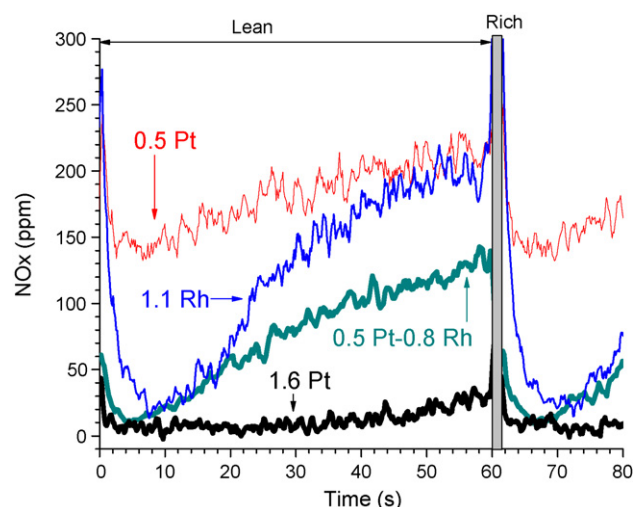
order of activity of the catalysts is 1.6Pt > 0.5Pt0.8Rh > 1.1Rh > 0.5Pt. However, if the NO_x storage performance of the catalysts are normalised on the basis of the ratio of exposed metal atoms (as determined from CO chemisorption) to total number of Ba atoms, then the order of activity becomes 0.5Pt (1.0) > 0.5Pt0.8Rh (0.18) > 1.1Rh (0.09) with the normalised NO_x storage performances given in brackets. (The 1.6Pt catalyst has been excluded from the comparison because normalization of catalytic data at high conversions introduces large errors.) Clearly, Pt is a much more active metal than Rh for NO_x storage reduction.

The plots in Fig. 2 showing the outlet concentration of NO_x over the course of 80 s provide some explanations for the differences in performances observed in Fig. 1.

The high activity of 1.6Pt is evident from the very low NO_x concentration in the reactor outlet. This contrasts with the poor performance of the 0.5Pt sample which gives a minimum NO_x concentration of 140 ppm after the reintroduction of the lean phase. The NO_x signal gradually increases as the catalyst becomes increasingly saturated with NO_x. The 1.1Rh catalyst shows a minimum NO_x concentration of 30 ppm 10 s after the switch to the lean phase but the poor performance of the catalyst thereafter is evident from the sharp increase in NO_x concentration exiting the catalyst bed. This suggests that the Rh is efficient in the reduction of NO_x but poor at storing it. The poor performance of the 1.1Rh catalyst in storing NO_x is also evident in the long tail of NO_x eluted for up to 10 s after the

Table 2
Catalyst characterisation

Catalyst	Code	Pt		Rh		M* (µmol/g$_{cat}$)	CO/M*	Ba	
		wt%	(µmol/g$_{cat}$)	wt%	(µmol/g$_{cat}$)			wt%	(µmol/g$_{cat}$)
Pt/Ba/γ-Al$_2$O$_3$	0.5Pt	0.52	27	–		27	0.15	16.4	1197
Pt/Ba/γ-Al$_2$O$_3$	1.6Pt	1.58	81	–		81	0.17	13.8	1007
Pt/Rh/Ba/γ-Al$_2$O$_3$	0.5Pt0.8Rh	0.49	25	0.79	77	102	0.41	15.4	1158
Rh/Ba/γ-Al$_2$O$_3$	1.1Rh	–	–	1.07	104	104	0.72	17.0	1278

M*: Pt, Rh or PtRh.

switch from rich to lean conditions. This can be attributed to NO_x released during the rich phase traveling more slowly through the catalyst bed than the components of the rich phase (CO and/or H_2) and not being stored quickly enough as the feed changes from rich to lean. Evidence for these chromatographic type effects have been presented recently [15].

The 0.5Pt0.8Rh catalyst has the beneficial property of Rh which imparts good NO_x reduction activity as evidenced by the low concentration of NO_x exiting the catalyst just after the switch to lean. Thereafter, the concentration of NO_x increases due to a decrease in the rate of trapping due to the progressive saturation of the catalyst. The presence of Pt is clearly beneficial in ensuring that the rate of increase in levels of NO_x is not as marked as with 1.1Rh.

The high temporal resolution, fast switching and use of isotopically labelled ^{15}NO allowed detailed analysis of the regeneration phase of the cycles. Fig. 3 shows the evolution of the gases during regeneration at 350 °C. $^{15}N_2$, ^{15}NO and $^{14}NH_3$ were the only gases detected during the regeneration. There was no signal at $m/e = 46$ for $^{15}N_2O$. It should be noted that the signal for $^{14}NH_3$ and $^{15}N_2$ were obtained from different cycles during the same experiment. Initially, the catalyst was exposed to ^{14}NO for 18 cycles, then the feed was switched to ^{15}NO. The $^{14}NH_3$ signal was obtained during cycle number 18, whereas that of $^{15}N_2$ was obtained during cycle number 40. Fig. 1 shows, that the NO_x storage from cycle 10 to 40 does not change and independent experiments with ^{14}NO for 40 cycles showed that

the signal for $^{14}NH_3$ did not change significantly from cycle 10 to 40.

There are some interesting features in Fig. 3, the most notable of these is the double $^{15}N_2$ peak. Fig. 3A shows that a small peak of $^{15}N_2$ was produced upon introduction of the regeneration mix over the 0.5Pt catalyst. The signal then returned to the baseline before rising sharply after 1.2 s at the point where the regeneration mix was replaced by the lean mix. Ammonia appeared 0.6 s after the switch to rich conditions and it reached a peak value after 1.2 s before decreasing to the baseline. Increasing the Pt loading (from 0.5 to 1.6 wt%), resulted in significant increase in the area of the first $^{15}N_2$ peak (from 0.03 to 0.80 μmol) (Fig. 3B and Table 3), whereas the amount of $^{15}N_2$ released during the second peak remained the same as that observed for the 0.5Pt sample ($\sim$0.29 ± 1 μmol). A small ammonia peak was also evident for 1.6Pt; it appeared 1.1 s after introduction of the rich phase. For both Pt catalysts, the quantity of NO released during the rich phase was almost negligible (0.02 ± 1 μmol).

For the 1.1Rh sample (Fig. 3C), as seen with 1.6Pt, there was a double peak of $^{15}N_2$ and a peak of $^{14}NH_3$. However, the relative ratios of the peaks differ and the Rh catalyst produces more NH_3.

The bimetallic 0.5Pt0.8Rh catalyst displays some distinctive differences as compared to the 0.5Pt material. In particular, the addition of 0.8Rh to the 0.5Pt catalyst results in the appearance of a much larger first peak of $^{15}N_2$ (0.50 μmol) compared to 0.5Pt (0.03 μmol). Thus the addition of Rh promotes the initial reduction of NO_x upon switching from lean to rich. The quantity of N_2 eluted in the second peak was almost identical to that observed over 0.5Pt ($\sim$0.29 μmol). However, Fig. 3B shows that this is not specific to Rh because of the addition of extra Pt to the 0.5Pt to form the 1.6Pt material results in an even greater evolution of $^{15}N_2$ immediately after the switch to rich conditions. For the 1.1Rh sample the evolution of N_2 in the second peak was lower than that observed for the Pt-containing catalysts (Table 3).

It is interesting to note that ammonia was produced in all cases, typically showing a delay of $\sim$0.6 s after switching in the rich feed, peaking at $\sim$1.2 s, before declining to the baseline after $\sim$2.0 s. Thus ammonia was produced, desorbed or more likely continuously adsorbed/desorbed along the length of the catalyst bed for $\sim$0.8 s after the switch from rich to lean. The adsorption/desorption could occur on exposed Bronsted and Lewis acid sites on uncovered Al_2O_3. Similarly, nitrogen was produced in the absence of reductant for almost 1 s after the switch to lean conditions but only when rhodium is present.

3.3. Catalytic results at 250 °C

Lowering the reaction temperature produced significant differences in the results as can be seen in Fig. 4. For the 1.6Pt catalyst there was a clear decrease in the amount of NO_x stored on the catalyst from one cycle to the next over the first 15 cycles. For example, when using 4.5% CO + 1.5% H_2 as reductant, the initial 70% of NO_x stored decreased to 21% after 45 cycles. For the bimetallic 0.5Pt0.8Rh catalyst, the storage of
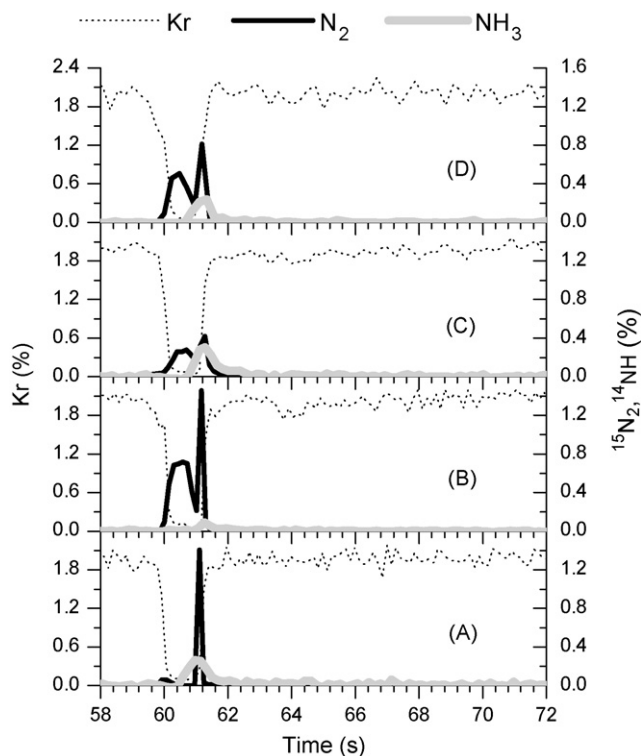

Fig. 3. Evolution of $^{15}N_2$, $^{14}NH_3$ and Kr as a function of time using a 1.2 s rich switch with (H_2 + CO + CO_2 + H_2O) for (A) 0.5Pt; (B) 1.6Pt; (C) 1.1Rh; (D) 0.5Pt0.8Rh.

Table 3
NO stored during 60 s lean period and N released during regeneration phase (4.5% CO + 1.5% H_2 + 10% CO_2 + 10% H_2O) over various catalysts at 350 °C

Catalyst	Regeneration conditions	Lean (μmol)	Regeneration (μmol)					
		NO stored	N_2 peak 1	N_2 peak 2	N_2 total	NH_3	N_2O	NO
0.5Pt	1.2 s rich	0.95	0.03	0.28	0.31	0.30	0.00	0.03
1.6Pt	1.2 s rich	2.30	0.80	0.30	1.09	0.10	0.00	0.01
1.1Rh	1.2 s rich	1.45	0.41	0.11	0.52	0.34	0.00	0.07
0.5Pt0.8Rh	1.2 s rich	1.81	0.50	0.29	0.79	0.22	0.00	0.01

NO_x after 45 cycles was almost identical to that observed for 1.6Pt. However, the initial activity was lower (53%), indicating that the rate of deactivation from one cycle to the next was lower for the bimetallic catalyst. The monometallic 1.1Rh material showed poor initial storage (20%) but reasonably good
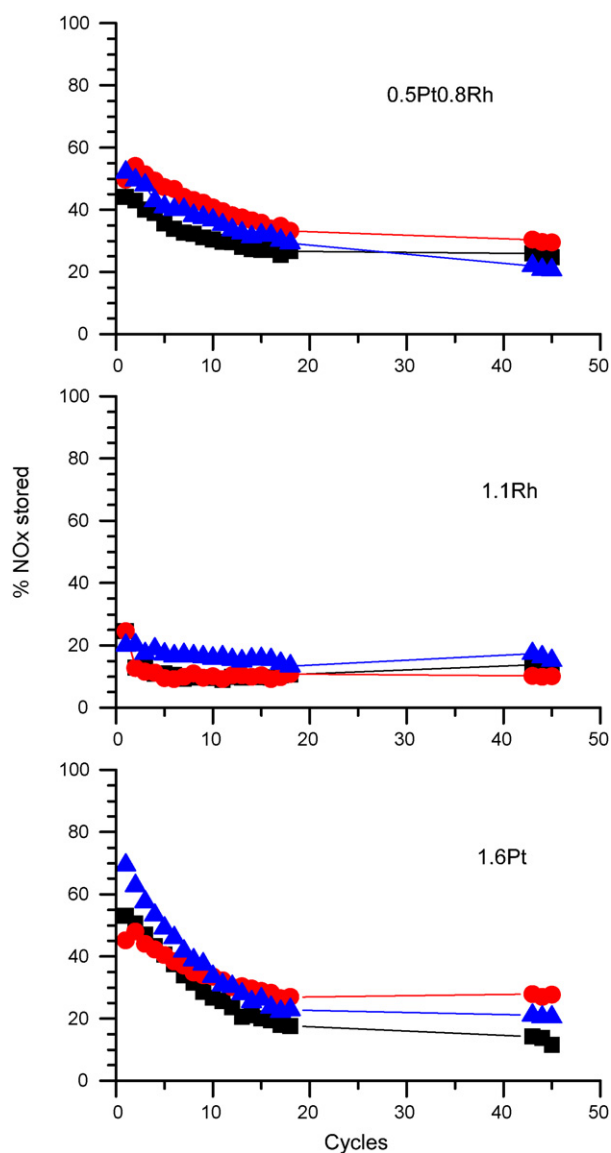

Fig. 4. NO_x storage as a function of the number of lean/rich cycles at 250 °C for the three catalysts with different regeneration mixes; 6% H_2 (●); 4.5% CO + 1.5% H_2 (▲) and 6% CO (■). All regeneration mixes also contained 10% CO_2 and 10% H_2O.

stability from one cycle to the next, giving a storage of NO_x of 16% after 45 cycles.

The same trends were observed for the different reductant mixes over the three catalysts. For the Rh-containing catalysts there was no significant effect of reductant on the final catalyst performance. For 1.6Pt the final NO_x catalyst performance was in the order 6% H_2 > 1.5% H_2 + 4.5% CO > 6% CO, with the difference in activity between 6% H_2 and 6% CO being 15%.

If the performance of the catalysts is evaluated on the basis of the ratio of exposed metal atoms to total Ba atoms (Table 2) then the order of reactivity is 1.6Pt > 0.5Pt0.8Rh > 1.1Rh. The order of reactivity remains the same regardless of the regeneration mix used, however, the Rh-containing catalysts compared more favourably with the 1.6Pt catalyst when CO was included in the regeneration mix.

Fig. 5 shows the evolution of nitrogen, nitrous oxide and ammonia during a typical lean/rich/lean cycle for the 0.5Pt0.8Rh catalyst as a function of different rich phases. The start of the rich phase was marked by a decrease in the signal of the Kr tracer and the end of the rich phase by an increase in the Kr signal.

Similarly to the results at 350 °C, nitrogen evolved in two distinct peaks. The start of the first release of nitrogen coincided with the start of the rich phase. The start of the second nitrogen peak coincided with the switch back to lean conditions and in many cases nitrogen production continued for at least 1 s into the lean phase following the rich phase.

Table 4 shows that the amount of $^{15}N_2$ evolved was dependent on the reductant used and was in the order: 6% CO > 4.5% CO/1.5% H_2 > 6% H_2. Even though 6% H_2 regenerated the catalyst most efficiently, the selectivity to $^{15}N_2$ formation was low. Ammonia production accounted for the majority of N released during the regeneration phase when using 6% H_2 but decreased markedly with decreasing H_2 content in the regeneration mix. It is interesting to note that despite the absence of H_2 in the 6% CO regeneration mix it was still possible to produce some ammonia.

When 6% H_2 was used as a reductant, evolution of ammonia occurred just after the transition from lean to rich and continued for up to 4 s into the subsequent lean phase. When CO was present in the regeneration mix, evolution of ammonia was delayed to ~1 s after the switch from lean to rich and continued for up to 1 s into the lean phase.

In contrast to the results at 350 °C, nitrous oxide was a significant product at 250 °C but only when CO was present in the regeneration mix. No nitrous oxide was detected when 6% H_2 was used as a reductant. The evolution of $^{15}N_2O$ followed a
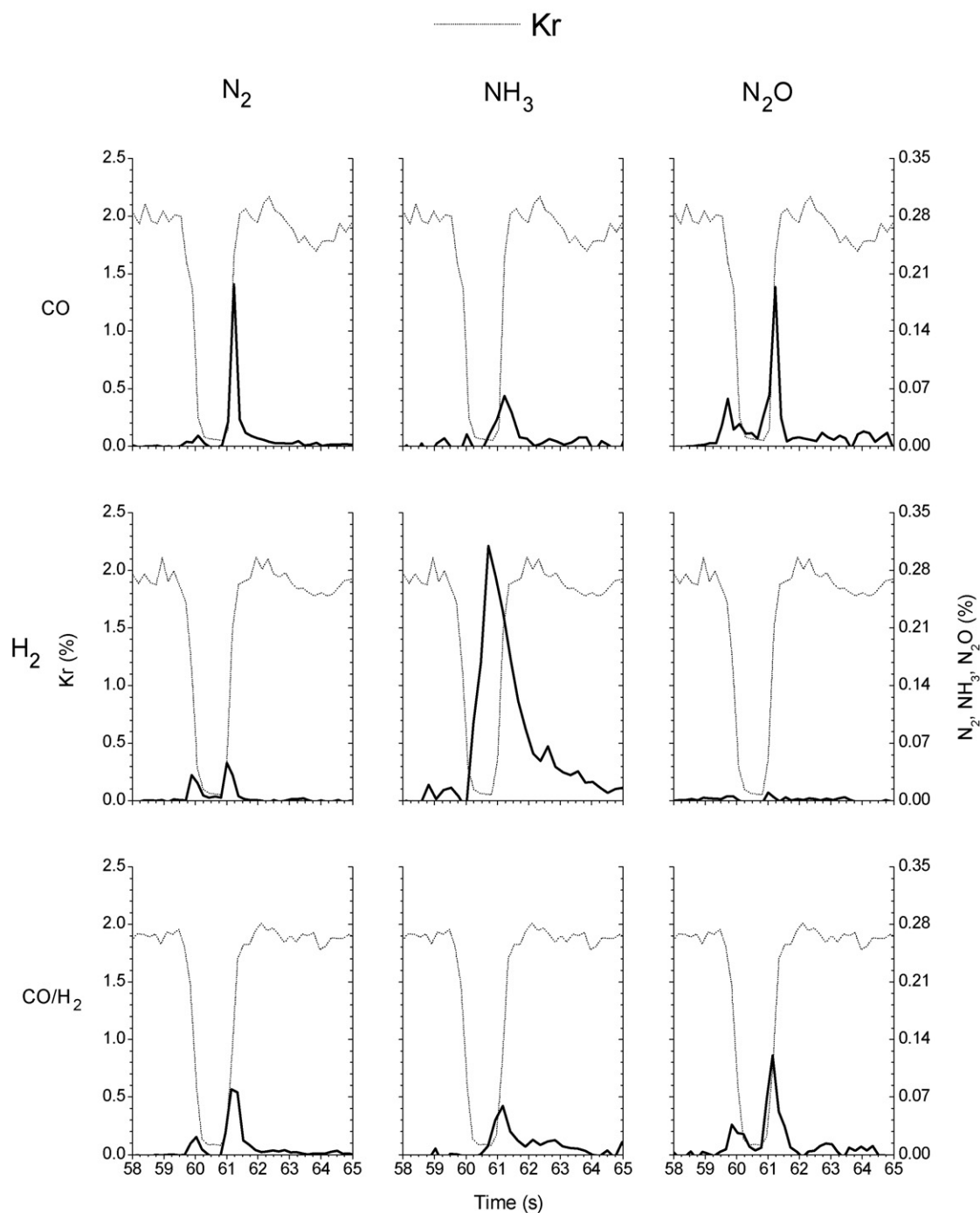
Fig. 5. Evolution of $^{15}N_2$, $^{15}N_2O$, $^{14}NH_3$ and Kr (dotted line) as a function of time at 250 °C during a lean/rich/lean cycle with a rich phase containing 6% CO, 6% H_2 or 1.5% H_2 + 4.5% CO over the 0.5Pt0.8Rh catalyst. All rich feeds also contained 10% CO_2 and 10% H_2O.

Table 4
NO stored during 60 s lean period and N released due to regeneration over 0.5Pt0.8Rh at 250 °C

Catalyst	Lean (μmol)	Regeneration (μmol)							
	NO stored	N_2 peak 1	N_2 peak 2	N_2 total	NH_3	N_2O peak 1	N_2O peak 2	N_2O total	NO
CO	0.62	0.01	0.10	0.11	0.06	0.04	0.11	0.15	0.03
H_2	0.73	0.02	0.02	0.04	0.64	0.00	0.00	0.00	0.01
H_2/CO	0.48	0.01	0.06	0.07	0.12	0.03	0.07	0.10	0.02

very similar trend to that of $^{15}N_2$, being evolved in two peaks at the interfaces between the phases. The selectivity to $^{15}N_2O$ was slightly greater than to $^{15}N_2$ production when using the CO-containing reductants.

4. Discussion

The use of isotopically labelled ^{15}NO and fast transient switching between lean and rich conditions has provided some important insights into the NO_x reduction process with Pt and Rh-promoted Ba/Al_2O_3 catalysts. These are discussed under the following headings:

4.1. Equilibrium between storage and reduction

The short but realistic regeneration (1.2 s) and storage times (60 s) used in this study have highlighted the importance of the relationship between rates of regeneration and storage in determining the overall performance of the Pt and Rh based NO_x storage catalysts. This is particularly evident at 250 °C. For the 1.6Pt catalyst at 250 °C there was a marked decrease in NO_x storage from one lean/rich cycle to the next until a steady state was attained. Scholz et al. [29] noted similar decreases in performance of their $Pt/Ba/Al_2O_3$ catalyst as a function of the number of cycles. However, they attributed decreasing performance to decreases in the BET surface area and Pt dispersion. In our case, by carrying out the pre-conditioning described in the experimental section after running a series of NSR cycles, the catalyst activity could be completely recovered, ruling out any significant changes in metal dispersion or BET surface area. In addition, the decrease in performance was most apparent at lower temperatures (compare Figs. 1 and 4) where sintering is not likely to be a problem.

The explanation for the decreasing performance in our case lies in the difference in rates of NO_x storage and reduction. Pt is a good oxidation catalyst and can rapidly convert NO to NO_2 which is subsequently stored predominantly as nitrates [30] and so the initial NO_x uptake is very good. However, the performance of the catalyst decreases rapidly at low temperature (250 °C). This can be attributed to incomplete regeneration of the catalyst.

On the other hand, the 1.1Rh catalyst gives almost complete regeneration as evidenced by the low level of NO exiting the catalyst bed immediately after regeneration at 350 and 250 °C (not shown here). The relatively stable NO_x storage from one cycle to the next at 250 and 350 °C in the case of the 1.1Rh catalysts strongly suggests that the rate of storage rather than the rate of regeneration is likely to be limiting the performance of the 1.1Rh catalyst. It appears that during the rich phase the Rh is sufficiently active to remove all the NO_x stored in the preceding lean phase, thus completely regenerating the catalyst for the subsequent lean phase.

The poor performance of the Rh catalyst in storing NO_x has also been noted by Abdulhamid et al. [17]. They attributed this to the lack of spillover of NO_x from Rh to the storage sites. Alternatively, it could simply be that Rh is a poor oxidation catalyst. This view is supported by the work of Schattler and Taylor [31] in three way catalysis (TWC) which shows that under transient conditions Rh also has very poor oxidation activity for CO and hydrocarbons.

Ideally the bimetallic catalyst 0.5Pt0.8Rh should combine the beneficial effects of Pt for storage and Rh for reduction. However, this is not apparent at 350 °C where the performance of the bimetallic 0.5Pt0.8Rh is poorer than the 1.6Pt (Fig. 1), despite the fact that CO chemisorption results suggest that the dispersion of Pt is lower than that of Pt and Rh in the bimetallic catalyst (Table 2). At 250 °C, the final performance of the bimetallic catalyst is slightly higher than the 1.6Pt. However, if the performance is compared on the basis of the ratio of exposed metal atoms to Ba atoms then the Pt catalyst outperforms both the Rh-containing catalysts. Clearly, in our case the addition of Rh does not have a beneficial effect at either of the temperatures investigated.

In summary, over a clean NSR catalyst, the initial performance is determined solely by the rate of NO_x storage. If the rate of regeneration during the rich phase is not sufficiently fast to fully remove all the NO_x stored in the previous lean phase, then levels of stored (unreduced) NO_x will gradually increase from one cycle to the next, resulting in deteriorating performance of the catalysts. This will proceed until an equilibrium point is achieved at which the amount of N atoms stored during the lean phase exactly matches the amount of N released during regeneration. At this steady state point the performance of the catalyst from one cycle to the next remains constant. This describes well the process occurring over the monometallic Pt catalysts. If on the other hand, the rate of regeneration is sufficiently fast then all the NO_x stored in the preceding lean phase will be removed during the subsequent rich phase. In this case there will be no deactivation from one cycle to the next and the performance of the catalyst is determined by the rate of storage during the lean phase. This describes the process occurring over the monometallic 1.1Rh catalyst.

4.2. The evolution of products

The evolution of products during the regeneration process is complex and very much dependent on the temperature and composition of the reductant phase. However, the following points can be distilled from the data presented here:

(a) Nitrogen formation occurred in two stages, resulting in two nitrogen peaks. The first peak of nitrogen occurred instantaneously upon introduction of the rich mix. The second peak of nitrogen always coincided with the point at which the rich phase was replaced by the lean phase.

(b) Ammonia was produced to varying degrees at 350 °C; typically for 1.2 s H_2 + CO regeneration mixes, ammonia production started roughly 0.6 s after the switch to rich and peaked at ~1.2 s.

(c) Ammonia was also produced at 250 °C, to a much greater extent when there was no CO in the reductant mix.

(d) Nitrous oxide was produced at 250 °C but not at 350 °C. The evolution of nitrous oxide closely matched that of nitrogen, at the interfaces between the lean and rich phases.

(e) Nitrogen and ammonia were detected in the gas stream up to 4 s after the switch back to lean conditions, providing evidence for continued reduction of NO_x under lean conditions.

The evolution of the first peak of nitrogen and nitrous oxide (at 250 °C) occurred instantaneously upon the switch to rich conditions and can be attributed to direct reaction of NO_x with either CO or H_2 on a reduced metal surface. These reactions are well known to occur over Pt and Rh based catalysts in the 250–350 °C temperature range [32]. For Pt catalysts, Burch and Millington [33] proposed that the role of the reductant is to reduce PtO_x to Pt^0 which can then dissociate NO, the adsorbed N atoms then combining to form gaseous nitrogen. They showed under transient TAP conditions that the yield of N_2 was comparable for the $NO + H_2$ and $NO + CO$ reactions. The formation of N_2O can proceed via the coupling of N_{ads} and NO_{ads} or through an adsorbed $(NO)_2$ dimer species [2,34]. Metallic rhodium can also dissociate NO, leading to N_2 formation via a similar mechanism to that proposed over Pt [32,35]. Similarly N_2O can be formed over reduced Rh based catalysts via reaction of NO_{ads} with N_{ads} [35]. The rate of reduction of either PtO_x or RhO_x is likely to be fast under the rich conditions present during the regeneration phase at 250 and 350 °C. Once Pt and/or Rh are reduced, the route to either N_2 or N_2O (at lower temperatures) via NO dissociation is facile.

With regard to the formation of ammonia, the results in Figs. 3 and 5 show that ammonia is evolved in all cases. In most cases the evolution occurs roughly 0.6 s after the switch to rich conditions, at the point at which nitrogen levels started to decrease or have returned to the baseline. The exception to this occurs when using 6% H_2 as reductant at 250 °C. In this case ammonia evolution occurred almost immediately after introducing the reductant. These results can be explained by the relative concentrations of stored NO_x and added H_2. Cumaranatuge et al. [36] have suggested that the evolution of ammonia is dependent on the local NO_x/H_2 ratio so that in regions where the H_2 level is high compared to NO_x, the reaction with the released NO_x will form mostly NH_3. This view is supported by Sakamoto et al. [13], who also showed using a TAP-type reactor that large quantities of NO_x and the products of reduction are evolved almost instantaneously (within 5 ms at $T > 300$ °C) upon introduction of H_2.

The mechanism by which the NO_x is reduced is open to debate. For example, Liu and Anderson [20] and Fanson et al. [37] have proposed that the reductant is activated on the metal site and spills over onto the support where it interacts with the stored NO_x resulting in release of NO_x. Nova et al. [38] suggest that in addition to spillover, migration of mobile nitrate species to the Pt metal site should also be considered. Zhou et al. [39] suggest that nitrate ions are extremely mobile and can migrate to the Pt sites to be reduced. This view is supported by *ab initio* molecular dynamic simulations which show that in theory nitrates and nitrites can diffuse rapidly across a BaO surface [40].

The fact that we observe the formation of large amounts of ammonia shows that the conditions at the catalytically active sites on the catalyst during the reduction of stored NO_x must be

consistent with a high hydrogen to NO_x ratio. This is most easily understood if we assume that migration of NO_x to the metal/support interface is fast compared to spillover of reductant from the metal to the support. On this basis we suggest that in the first few milliseconds after introduction of the rich phase the metallic sites are reduced but then immediately exposed to a high concentration of NO_x, favouring the formation of nitrogen and nitrous oxide (at 250 °C) rather than ammonia. As the concentration of NO_x decreases (due possibly to slower diffusion of more strongly bound NO_x or of NO_x that is more remote from the metal), the ratio of NO_x/H_2 decreases and ammonia formation becomes favoured.

The only exception to this that we have observed is the case where 6% H_2 was used as a reductant at 250 °C. In this case the ratio of H_2/NO_x was initially high and ammonia (in addition to nitrogen) was formed immediately after introduction of the rich phase.

The formation of ammonia when 6% CO was used as a reductant (at 250 °C) suggests that the direct reaction of NO with H_2 in the rich phase is not the only route to ammonia formation. Hydrogen that is required for the formation of ammonia could be produced from CO and H_2O via the water gas shift reaction (WGS), Epling et al. [41] have shown that NSR catalysts can have some activity for the water gas shift reaction even at temperatures as low as 200 °C. Alternatively, Lesage et al. [23] and Szailer et al. [24] suggest that ammonia can be formed via the reaction of NO and CO to form isocyanates which are readily hydrolysed to form ammonia.

Ammonia production extends for several seconds after reintroduction of the lean phase. It is hard to imagine a process whereby ammonia could be formed under lean conditions, so instead we suggest that ammonia formed during the rich phase slowly desorbs from the surface of the catalyst after the switch to lean. Further evidence for a stored reductant comes from the evolution of the second nitrogen peak initiated by the switch to lean conditions. This nitrogen peak can extend for several seconds into the lean phase. This peak can be attributed to any one of the following reactions:

- Selective oxidation of ammonia to nitrogen.
- Reaction of stored ammonia or isocyanates with stored NO_x. Lesage et al. [23] and Szailer et al. [24] have both shown that ammonia can react with stored nitrates to form nitrogen under reducing conditions. Under our conditions, the reaction between nitrates and stored ammonia could extend into the lean phase.
- Reaction of stored ammonia or isocyanates with gas phase NO_x present in the lean phase.

It is interesting to note that the majority of products are evolved at the lean/rich interfaces. This is true even when the rich duration is increased (result not shown here). Cummaranatunge et al. [36] have stressed the importance of the regeneration front as the rich phase moves through the bed. Our study, emphasises the importance of a second regeneration front as the lean phase following the rich phase passes over the reduced catalyst. In this zone, ammonia formed and stored as

the rich phase moved through the bed is converted to nitrogen (and nitrous oxide at low temperature).

5. Conclusions

The use of lean and rich phase durations and gas compositions similar to those experienced in real exhaust systems has enabled investigation of the key parameters involved in the NSR reaction over Pt and Rh based NSR catalysts. The coupling of fast switching and analysis and the use of ^{15}NO as a feed has allowed detailed analysis of the evolution of all the products and reactants of the regeneration within the short 1.2 s time frames typical of the rich phase. The following are the key findings from this work:

- For the monometallic 1.6%Pt/Ba/Al$_2$O$_3$ (at 250 °C) and bimetallic Pt/Rh/Ba/Al$_2$O$_3$ (at 250 and 350 °C) catalysts in this study the rate of regeneration during the rich phase was not sufficiently fast to fully remove all the NO$_x$ stored in the previous lean phase, resulting in deteriorating performance of the catalysts until an equilibrium point between the rates of reduction and storage was reached.
- In contrast, for the monometallic Rh/Ba/Al$_2$O$_3$ catalyst (at 250 and 350 °C) the rate of regeneration was sufficiently fast to remove the NO$_x$ stored in the preceding lean phase. In this case there was no deactivation from one cycle to the next and the performance of the catalyst was determined by the rate of storage during the lean phase.
- During regeneration, nitrogen was evolved in two peaks, the first peak occurred immediately upon the switch from lean to rich conditions. The second peak started at the point at which the gases switched from rich to lean.
- The first nitrogen peak can be attributed to direct reaction of reductant with NO$_x$ on a reduced Pt and/or Rh surface. The second N$_2$ peak occurring upon introduction of the lean phase can be explained by reaction of stored ammonia with stored NO$_x$ and/or by reaction with gas phase oxygen and/or NO$_x$ with the ammonia being formed either by hydrolysis of isocyanates or by direct reaction of NO and H$_2$.
- For the catalysts with similar molar metal loadings, the monometallic Pt-containing catalyst outperformed the monometallic Rh-containing one. The relatively poor performance of the Rh-containing catalyst can be attributed primarily to poorer activity for NO$_x$ storage.

Acknowledgement

References

[1] N. Takahashi, H. Shinjoh, T. Iijima, T. Suzuki, K. Yamazaki, K. Yokota, H. Suzuki, N. Miyoshi, S. Matsumoto, T. Tanizawa, T. Tanaka, S. Tateishi, K. Kasahara, Catal. Today 27 (1996) 63–69.
[2] R. Burch, Catal. Rev.-Sci. Eng. 46 (2004) 271–333.
[3] T. Lesage, J. Saussey, S. Malo, M. Hervieu, C. Hedouin, G. Blanchard, M. Daturi, Appl. Catal. B: Environ. 72 (2007) 166–177.
[4] W.S. Epling, G.C. Campbell, J.E. Parks, Catal. Lett. 90 (2003) 45–56.
[5] T.J. Toops, D.B. Smith, W.S. Epling, J.E. Parks, W.P. Partridge, Appl. Catal. B: Environ. 58 (2005) 255–264.
[6] R.J. Hendershot, R. Vijay, C.M. Snively, J. Lauterbach, Appl. Surf. Sci. 252 (2006) 2588–2592.
[7] N. Takahashi, K. Yamazaki, H. Sobukawa, H. Shinjoh, Appl. Catal. B: Environ. 70 (2007) 198–204.
[8] Y.J. Li, S. Roth, J. Dettling, T. Beutel, Top. Catal. 16 (2001) 139–144.
[9] W.S. Epling, A. Yezerets, N.W. Currier, Catal. Lett. 110 (2006) 143–148.
[10] J.S. Choi, W.P. Partridge, C.S. Daw, Appl. Catal. A-Gen. 293 (2005) 24–40.
[11] P. Koci, M. Schejbal, J. Trdlicka, T. Gregor, M. Kubicek, M. Marek, Catal. Today 119 (2007) 64–72.
[12] V. Medhekar, V. Balakotaiah, M.P. Harold, Catal. Today 121 (2007) 226–236.
[13] Y. Sakamoto, T. Motohiro, S. Matsunaga, K. Okumura, T. Kayama, K. Yamazaki, T. Tanaka, Y. Kizaki, N. Takahashi, H. Shinjoh, Catal. Today 121 (2007) 217–225.
[14] D. James, E. Fourre, M. Ishii, M. Bowker, Appl. Catal. B: Environ. 45 (2003) 147–159.
[15] J.P. Breen, C. Rioche, R. Burch, C. Hardacre, F.C. Meunier, Appl. Catal. B: Environ. 72 (2007) 178–186.
[16] H. Abdulhamid, E. Fridell, M. Skoglundh, Top. Catal. 30-31 (2004) 161–168.
[17] H. Abdulhamid, E. Fridell, M. Skoglundh, Appl. Catal. B: Environ. 62 (2006) 319–328.
[18] T. Szailer, J.H. Kwak, D.H. Kim, J. Szanyi, C.M. Wang, C.H.F. Peden, Catal. Today 114 (2006) 86–93.
[19] S. Poulston, R.R. Rajaram, Catal. Today 81 (2003) 603–610.
[20] Z.Q. Liu, J.A. Anderson, J. Catal. 224 (2004) 18–27.
[21] P. Jozsa, E. Jobson, M. Larsson, Top. Catal. 30–31 (2004) 177–180.
[22] N.W. Cant, M.J. Patterson, Catal. Lett. 85 (2003) 153–157.
[23] T. Lesage, C. Verrier, P. Bazin, J. Saussey, M. Daturi, Phys. Chem. Chem. Phys. 5 (2003) 4435–4440.
[24] T. Szailer, J.H. Kwak, D.H. Kim, J.C. Hanson, C.H.F. Peden, J. Szanyi, J. Catal. 239 (2006) 51–64.
[25] S.I. Matsumoto, Catal. Today 90 (2004) 183–190.
[26] H. Abdulhamid, J. Dawody, E. Fridell, M. Skoglundh, J. Catal. 244 (2006) 169–182.
[27] A. Amberntsson, E. Fridell, M. Skoglundh, Appl. Catal. B: Environ. 46 (2003) 429–439.
[28] H.F.J. Van't Blik, J.B.A.D. Vanzon, T. Huiznga, J.C. Vis, D.C. Koningsberger, R. Prins, J. Phys. Chem. 87 (1983) 2264–2267.
[29] C.M.L. Scholz, V.R. Gangwal, J.H.B.J. Hoebink, J.C. Schouten, Appl. Catal. B: Environ. 70 (2007) 226–232.
[30] L. Olsson, E. Fridell, J. Catal. 210 (2002) 340–353.
[31] J.C. Schlatter, K.C. Taylor, J. Catal. 49 (1977) 42–50.
[32] K.C. Taylor, Catal. Rev.-Sci. Eng. 35 (1993) 457–481.
[33] R. Burch, P.J. Millington, Catal. Today 26 (1995) 185–206.
[34] R. Burch, A.A. Shestov, J.A. Sullivan, J. Catal. 188 (1999) 69–82.
[35] P. Granger, F. Dhainaut, S. Pietrzik, P. Malfoy, A.S. Mamede, L. Leclercq, G. Leclercq, Top. Catal. 39 (2006) 65–76.
[36] L. Cumaranatunge, S.S. Mulla, A. Yezerets, N.W. Currier, W.N. Delgass, F.H. Ribeiro, J. Catal. 246 (2007) 29–34.
[37] P.T. Fanson, M.R. Horton, W.N. Delgass, J. Lauterbach, Appl. Catal. B: Environ. 46 (2003) 393–413.
[38] I. Nova, L. Lietti, L. Castoldi, E. Tronconi, P. Forzatti, J. Catal. 239 (2006) 244–254.
[39] G. Zhou, T. Luo, R.J. Gorte, Appl. Catal. B: Environ. 64 (2006) 88–95.
[40] P. Broqvist, I. Panas, H. Gronbeck, J. Phys. Chem. B 109 (2005) 15410–15416.
[41] W.S. Epling, A. Yezerets, N.W. Currier, Appl. Catal. B: Environ. 74 (2007) 117–129.